

Municipal bond volatility spillover modeling with COVID-19 effects by hybrid integration of GARCH and machine learning: The connectedness of U.S. states and South African bond markets

Gordon Dash

University of Rhode Island, USA

Nina Kajiji

University of Rhode Island, USA, and
The NKD-Group, Inc., USA

Helper Zhou

Durban University of Technology, Durban, SA

Domenic Vonella

Refinitiv, A London Stock Exchange Group, USA

Keywords

COVID-19, Machine learning, South African bond market, U.S. municipal bond markets

Abstract

After the passage of the United States Africa Growth and Opportunity Act (AGOA), the emerging market economy of South Africa (SA) recorded substantial increases in duty-free exports to the U.S. Any loss or disruption of AGOA privileges could undermine SA as a trade partner with designated states in the U.S. For U.S. states most affected by the passage of the 2017-2018 Tax Cuts and Jobs Act (e.g., SALT states) along with the COVID-19 pandemic effects, the elimination of the tax exemption impacted how state governments assist in funding international trade. This paper presents a novel hybrid EGARCH conditional volatility and artificial neural network model to map the COVID-19 effect on volatility spillovers between the SA government bond market and state-issued U.S. municipal bonds traded in secondary markets. Our empirical investigation provides three innovations. First, this study addresses illiquidity and informed trading impairments by observing over 11.5 million municipal bond trades. Second, we provide new evidence that a radial basis function artificial neural network enhanced by conditional volatility and fundamental factors can effectively map the geographical bond market spillover transmission between SA and individual U.S. states. Third, on state-based muni trades, we report how the AR (1) process is weighted positively across all East coast states during the global pandemic. Lastly, the study details how COVID-19 and South African conditional volatility impacted the returns of recorded trades of municipal bonds in SALT states. A global summary of the findings concludes with a discussion of how precious metals trading contributes to the performance of state-based municipal bonds.

1. Introduction

Over the last three decades, intercontinental financial markets' economic integration has grown in complexity. Since the mid-1980s, the literature has devoted itself to understanding the global financial integration of traded commodities as well as risk and return comovements (see, for example (Ando, 2019; Dizioli, Guajardo, Klyuev, Mano, & Raissi, 2016; Góes et al., 2017)). As to Africa, robust economic growth rates are needed to assist the roughly 40 percent of the population still living in poverty. One way to support African growth and opportunity is by increasing African engagement with the international economy through increased participation in international trade. To that end, in 2000, the former United States (U.S.) President Bill Clinton signed the Africa Growth and Opportunity Act (AGOA), which is scheduled to expire after two extensions in 2025. This Act gave African countries a competitive, or preferential, export edge to the U.S. for slightly more than 6,500 products. Promoting the "trade does not

aid" mantra, AGOA stands out for its regional approach to stimulating growth in the private sector of small and large African countries.

AGOA has faced threats. Under the administration of former U.S. President Donald J. Trump, tariffs were imposed on essential products (e.g., aluminum and steel). This outcome propagated a bilateral channel of financial contagion between U.S. states and South African trade markets (for discussion, see Rigobon (2002) and Roy and Roy (2017)). International volatility spillovers result from financial contagion. One U.S.-based financial market impacted by international spillovers is the U.S. municipal bonds (muni) market. The onset of the COVID-19 era represents an additional source of contagion for financial markets. By way of example, using an autoregressive distributed lag model, Shehzad, Xiaoxing, Bilgili, and Koçak (2021), find that COVID-19-related spillovers from the United Kingdom to the U.S. exacerbated financial instability in the U.S. The authors also find that Asian and African economic crises affected U.S. financial stability. Shahzad, Bouri, Kang, and Saeed (2021) extended the examination of the financial market spillover effect between COVID-19 and cryptocurrency regimes. Further evidence of how the U.S. economic slowdown caused by the COVID-19 pandemic impacted other non-financial global markets (e.g., energy) is provided by Wang and Xinyu (2021).

In 2017 a tax plan signed by former U.S. President Donald Trump limited the tax deduction on federal returns allowed taxpayers of high-tax states. More appropriately referred to as the Tax Cuts and Jobs Act (TCJA), a cap on the state and local income tax (SALT) deduction were set at \$10,000, where there was no limit previously.

In this paper, we seek to map the effects of sovereign and international return and volatility spillover on the U.S. muni market during the pandemic era. The study design focused on SALT states where personal tax obligations were impacted (increased) by approximately 4% (or higher) after the passage of the TCJA. The remainder of the paper is organized as follows. Section 2 of the paper provides the theoretical underpinnings of the K4-RANN. The study data and necessary transformations to reduce over 11 million trades to a daily timescale are presented in section 3. Section 4 offers the system of models needed to specify the spillover equation. Empirical results and policy implications are developed in section 5. A summary is provided in section 6.

2. Literature review

Our paper's primary goal is to analyze the international transmission of return and volatility spillovers between U.S. Municipal state bond markets and the South African government bond market. There is a growing need to understand the relationship between financial market spillovers and the global production network in a financially interconnected world economy. For example, di Giovanni and Hale (2021) attributed the global production network as the mechanism behind the transmission of U.S. stock market spillovers to world markets. More recent contributions to the literature provide new evidence on the importance of networks and machine learning in bond return and volatility predictability (e.g., see Bianchi, Büchner, and Tamoni (2021) on the performance of neural networks forecasts in time-varying risk aversion and uncertainty channels). But, models based on the stochastic volatility process, as first introduced with the ARCH model of Engle (1982) and the GARCH model of Bollerslev (1986), provide a record of performance that is equally impressive. To that end, the Exponential Generalized Autoregressive Conditional Heteroscedasticity (EGARCH) model proposed by Nelson (1991) is today one of the most widely used within the GARCH family of extensions. The EGARCH model was proposed to consider the leverage effects of price fluctuation on conditional variance (i.e., bad news outweighs good news and impacts price variability).

The success these two branches of volatility modeling accumulated has led to the investigation of hybrid approaches – models that combine GARCH family extensions with the mapping capabilities of an artificial neural network (ANN). Several good summaries of hybrid approaches are apparent in the literature. Extant research provides evidence that the artificial intelligence foundation of RANN methods is a viable alternative to the GARCH framework when modeling volatility spillover in European bond markets (Dash Jr. & Kajiji, 2008). Hence, in this study, we avoid presenting comparative redundancy. Instead, we draw upon extant findings from Mademlis and Dritsakis (2021). After providing a literature review on the hybrid modeling of conditional volatility, the authors study empirics using Italian stock

report the empirical effectiveness of regularized and Bayesian-enhanced networks when applied to sizeable municipal bond datasets to capture yields in a noisy dataset (Dash, Kajji, & Vonella, 2018; Raman & Leidner, 2018). For the twenty selected states, the MSRB trade tape is gleaned for trades within the sample period. Table 1 summarizes the trade selection criteria for this study. After data munging, we retain 11,346,101 trades for empirical estimation (see Figure 4).

1.	Select all bonds with an investment-grade credit rating
2.	Exclude bonds that are priced to PUT
3.	Exclude taxable bonds
4.	Exclude variable interest bonds
5.	Exclude zero-coupon bonds
6.	Exclude pre-refunded bonds
7.	Exclude bonds whose maturity date is not between one and thirty years

Table 1. Muni bonds selection criteria for the selected states

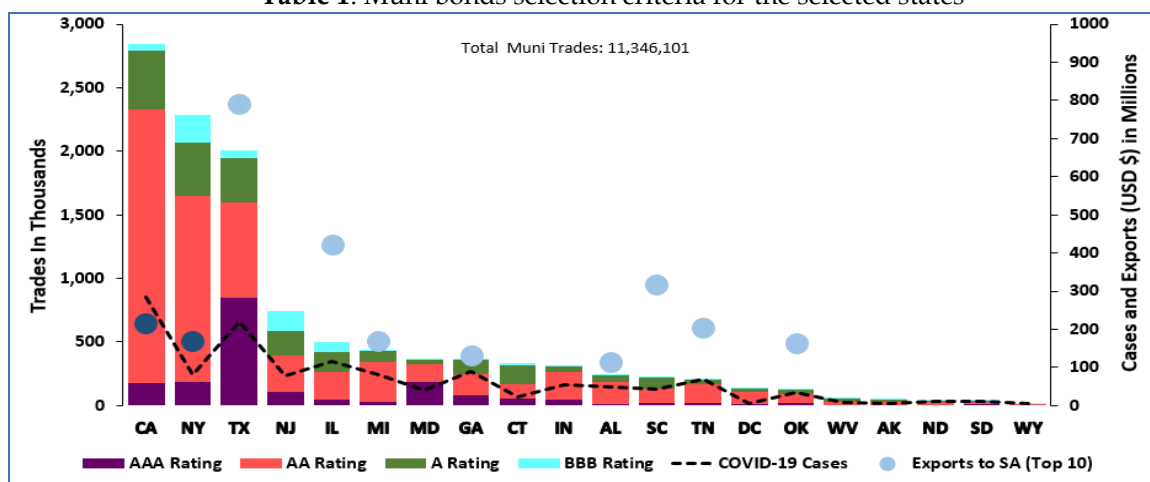


Fig. 2: Comparison of bond trades, total COVID-19 cases, and 2020 top 10 states with exports of NAICS total all merchandise to South Africa. Total muni trades are reported on the left axis. COVID-19 cases and exports are reported on the right axis. The two dark-colored dots signify states within the top 10 states with export relationship to SA belonging to the >8% SALT category, and the remaining belong to the 4%-8% SALT category.

The illiquid nature of the municipal bond market often results in very few trade observations for many bonds. Hence, it is helpful to treat bonds as homogeneous entities to construct a pooled statewide bond price. Also, because an individual bond in a given state can be traded several times during a trading day, we weigh each trade by the bond’s duration. Specifically, the weighted average bond price for state (*k*) bond (*i*) on the day (*t*) is computed using the following formulation.

$$WgDPrice_{k,i,t} = \left[\frac{P_{i,t} * S_{i,t}}{D_{i,t}} \right] \div 1000 \tag{1}$$

Where:

- $P_{i,t}$ = Trade price for bond *i* on day *t*
- $D_{i,t}$ = Duration for bond *i* on day *t*
- $S_{i,t}$ = Trade size of bond *i* on day *t*; $S = 1M$ for any trade size > 1M

Also, since a state may have multiple bonds traded on any given day, we compute an average bond trade price for the state (*k*) on day (*t*) as follows:

$$WgDPrice_{k,t} = \frac{1}{Q_{k,t}} \sum_{i=1}^{Q_{k,t}} WgDPrice_{k,i,t} \tag{2}$$

where $Q_{k,t}$ is the number of traded bonds for a state (*k*) on a given day (*t*). For 01-Jan-2020 through 20-Oct-2022, the pooling results in a sample size of 711 observations for 20 states.

3.3 Policy features

In ML studies, independent variables are supervisory variables referred to as features. An efficient solution to an econometric or machine learning modeling process requires careful feature selection. However, ML often depends on feature engineering to better understand the data, including additional and reformulated variables.

3.3.1 Sovereign bond indices.

Exposure to Treasuries, particularly long-term U.S. Treasury bonds, is proxied by capturing the *iShares 20+ Year Treasury Bond ETF* (TLT). The ETF is defined by bonds with remaining maturities greater than twenty years. The South African bond market is represented in the study by including the *South Africa 10-Year Bond Yield* (10YrSA). The data is from Investing.com. Additionally, two proxy variables were obtained representing the risk-free rates for the U.S. and South Africa. These are the *PIMCO 25+ Year Zero Coupon U.S. Treasury Index ETF* (ZROZ) and the *3 Month SA Bond Yield* (3MthSA).

3.3.2 Precious metals.

Gold is often viewed as a reliable measure of global market sentiment among precious metals. In South Africa, gold accounts for about a third of all exports. Vuyyuri and Mani (2005) provide affirmative evidence of the significance of gold demand factors in South Africa. By extension, Erling (2016) reported sensitivity between the returns on precious metals and external factors (e.g., bond yields, equity prices, etc.). The asymmetric linkages among precious metals, equity, and bond yields given a shock to the underlying returns found that own-asset variances explain the negative direction of most forecast variance errors except for the response of the gold and silver linkage (Urom, Anochiwa, Yuni, & Idume, 2019). The gold-to-platinum ratio (GP) is the ratio of the CME COMEX continuous gold futures contract and the CME COMEX continuous platinum futures contract.

3.3.3 U.S. COVID-19 data

The COVID data was obtained from the World Health Organization (WHO). For this study, we computed the COVID indicator as the ratio between new deaths in the US and recent cases in the US.

3.4 Market returns

Before developing the modeling equations, we must compute the excess yields for both the feature and target variables. Specifically, the excess returns, R , for a state, k , on the day, t , was computed using the price (P) of ZROZ as

$$R_{k,t} = [\text{Ln}(WgDPrice_{k,t}) - \text{Ln}(WgDPrice_{k,t-1})] - [\text{Ln}(P_{ZROZ,t}) - \text{Ln}(P_{ZROZ,t-1})] \quad (3)$$

Similarly, the excess returns on both TLT and 10YrSA are computed. The U.S. excess return is derived by subtracting the U.S. Treasury Index ETF (ZROZ) return from the PIMCO 25+ Year Zero Coupon return. Excess returns for the South African (SA) government bond market are computed based on the 3 Month SA Bond Yield (3MthSA).

$$R_{US,t} = [\text{Ln}(P_{TLT,t}) - \text{Ln}(P_{TLT,t-1})] - [\text{Ln}(P_{ZROZ,t}) - \text{Ln}(P_{ZROZ,t-1})], \text{ and} \quad (4)$$

$$R_{SA,t} = [\text{Ln}(P_{10YrSA,t}) - \text{Ln}(P_{10YrSA,t-1})] - [\text{Ln}(P_{3MthSA,t}) - \text{Ln}(P_{3MthSA,t-1})] \quad (5)$$

Finally, the return on the GP ratio is computed as

$$R_{GP,t} = [\text{Ln}(GP_t) - \text{Ln}(GP_{t-1})] \quad (6)$$

4. Research methodology

4.1 EGARCH framework

The extraction of time-varying volatility of financial time series has primarily been linked to the ARCH model of Engle (1982) and Bollerslev (1986). Nelson (1991) proposed the exponential GARCH (EGARCH) model to allow for asymmetry effects between positive and negative asset returns. Recently updated literature and findings provided by Le and Kakinaka (2010) employs a two-stage GARCH methodology to explain how mean return and volatility spillover effects impact the U.S., Japan, and

China’s stock markets. Consistent with past literature, we define the conditional returns on the US government bond index as an AR(1)-EGARCH(1,1) process.

$$R_{US,t} = b_0 + b_1R_{US,t-1} + a_{US,t}, \text{ where } a_{US,t} = \sigma_{US,t}\epsilon_{US,t} \tag{7}$$

In this model, $\{\epsilon_{US,t}\}$ is a sequence of independent standardized Gaussian random variates and $\sigma_{US,t}^2$ is the conditional variance of $a_{US,t}$. Further, the conditional variance is estimated as follows.

$$\ln(\sigma_{US,t}^2) = \alpha_{0,US} + \alpha_{1,US} \frac{|a_{US,t-1}| + \gamma_{US} a_{US,t-1}}{\sigma_{US,t-1}} + \beta_{US} \ln(\sigma_{US,t-1}^2) \tag{8}$$

Here, γ_{US} parameter signifies the leverage effect of $a_{US,t-1}$.

Owing to relatively strong trade and investment linkage with the U.S. economy, we model return and volatility spillover transmission to the SA government bond market based on U.S. trade activity. Specifically, the equation (9) expresses the conditional excess returns for the aggregate South African bond market, $R_{SA,t}$ as a multi-factor AR(1)-EGARCH(1,1) by including innovations from equation (7).

$$R_{SA,t} = b_0 + b_1R_{SA,t-1} + b_2R_{US,t-1} + b_3\sigma_{US,t-1}^2 + a_{SA,t}, \text{ where } a_{SA,t} = \sigma_{SA,t}\epsilon_{SA,t} \tag{9}$$

In this form, the conditional mean of the SA excess bond return depends on its own lagged excess return ($R_{SA,t-1}$), the lagged U.S. excess return ($R_{US,t-1}$), and the spillover effect introduced by the U.S. idiosyncratic shock. The conditional variance for SA is estimated as follows.

$$\ln(\sigma_{SA,t}^2) = \alpha_{0,SA} + \alpha_{1,SA} \frac{|a_{SA,t-1}| + \gamma_{SA} a_{SA,t-1}}{\sigma_{SA,t-1}} + \beta_{SA} \ln(\sigma_{SA,t-1}^2) \tag{10}$$

4.2 The RANN framework

Some processes have complex data that defy the use of linear regression-based techniques. The literature shows that the application of a multivariate feedforward radial basis function (RBF) artificial neural network (RANN) is an excellent method to analyze nonlinear functionals expressed with correlated variables (Leon-Delgado, Praga-Alejo, Gonzalez-Gonzalez, & Cantú-Sifuentes, 2018). Generally, RANN mapping is based on partial information or learning by example.

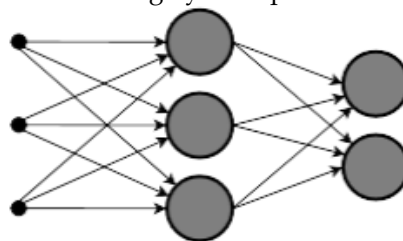


Fig. 3: Architecture of the multivariate RANN showing three inputs identified by small circles and two outputs

Fig. 3, shows a three-layer ($J_1 \rightarrow J_2 \rightarrow J_3$) feedforward neural network. Each node in the hidden layer uses a radial basis function, $\sigma(r)$, as its nonlinear activation function. Usually, the same RBF is applied on all nodes; hence, the RBF nodes have the nonlinearity $\phi_i(\vec{x}) = \phi(\vec{x} - \vec{c}_i), i = 1, \dots, J_2$, where \vec{c}_i is the center of the i -th node and $\phi(\vec{x})$ is an RBF. The RANN uses a linear optimization method and adjustable weights to achieve a globally optimal solution (Wu, Wang, Zhang, & Du, 2012).

Function approximation involves learning or approximating the underlying relationship from a given finite input-output data set

$$y(x) = f(x) + \epsilon \tag{11}$$

where $x \in R^{M \times 1}$ is an input vector, $f(\cdot)$ is the arbitrary nonlinear function unknown in the general case, and ϵ is the observed disturbance with unknown characteristics (Rudenko & Bezsonov, 2011).

4.3 The hybrid EGARCH-RANN framework

In the case of a multivariate specification (e.g., more than one target variable), where the multiple outputs rely upon a singularly defined feature set, mapping the hidden interaction among the multiple targets with the feature creates a more general relationship to the hidden node structure (Prathiba, BalasinghMoses, Devaraj, & Karuppasamyandiyana, 2016).

The hybrid multivariate (multiple target variables) specification of the EGARCH-RANN spillover model is presented in the equation (12). The RANN method does not consider any underlying probability distribution assumptions; hence, no distributional assumptions are made about v_t . Equation (12) follows for the <4% group.

$$(R_{1,t} \dots R_{N1,t}) = b_0 + b_1 \bar{R}_{t-1} + b_2 R_{US,t-1} + b_3 R_{SA,t-1} + b_4 Covid_{t-1} + b_5 GP_{t-1} + b_6 \sigma_{SA,t-1}^2 + \epsilon_{i,t}, \tag{12}$$

where: $\bar{R}_t = \sum_{i=1}^N w_i R_{i,t}$, and $w_i = \frac{\text{Total trades in State } i}{\text{Total trades in the sample}}$, $i = 1 \dots N1$, where $N1$ is the number of states in the <4% SALT category. Similarly, we define two more formulations of the equation (12). One for the 4%-8% and the other for the >8% SALT categories with $N2$ and $N3$. Hence, $N = N1 + N2 + N3 = 20$ states. The model system uses six feature variables. These are a lagged weighted average of the sample state excess returns (\bar{R}_{t-1}), the lagged excess returns TLT , lagged excess returns of the $SA10Yr$, the lagged COVID-19 survival ratio, and the spillover effect introduced from the SA idiosyncratic shock. Before implicating estimation methods, the data was de-correlated using the zero-phase component analysis (ZCA), aka ZCA Whitening (Chiu, 2019).

4.4 RANN spillover regression weights and model performance

Table 2 presents the estimated RANN weights for the feature variables ordered by the previously identified SALT categories (< 4%, 4% to 8 %, and > 8%).

4.4.1 K4-RANN model performance

Model performance (Table 2) across the three categories was strong. But the <4% category produced the weakest AIC metric among the three estimated models. With an AIC value of -4313.17, the performance in the <4% fell moderately short of -4934.74 and -5154.08, which were achieved in the 4% to 8% and >8% categories. This characterization of model performance strength is supported by the estimated MSE across categories: 0.0022, 0.0009, and 0.0007, respectively. The Modified Direction (M. Dir) performance metric offers insight into the overall strong performance across the three categories. At 96.7%, 96.1, and 95.8, it is evident that the mapping capabilities of the K4-RANN solutions are on par with one another.

SALT Category	State	Intercept	Lagged States (\bar{R}_{t-1})	Lagged USA ($R_{US,t-1}$)	Lagged SA ($R_{SA,t-1}$)	Lagged COVID ($Covid_{t-1}$)	Lagged GP (GP_{t-1})	Lagged SA Vol ($\sigma_{SA,t-1}^2$)
Less than 4%	AK	-0.1462	0.0262	-0.2183	-0.0914	-0.1139	0.3078	-0.2316
	IN	-0.0021	0.0528	0.0489	0.0804	-0.0669	-0.0296	0.0590
	ND	-0.1187	0.1218	-0.0656	0.0555	-0.0129	0.0484	0.0619
	SD	0.1708	0.2164	0.0624	0.1564	0.3271	0.0775	-0.0385
	WV	-0.0086	0.0589	0.0927	-0.0696	-0.1102	-0.2452	0.0391
	WY	-0.3002	-0.1478	0.0731	-0.0384	-0.2881	-0.0257	-0.0159
	Avg.	-0.0675	0.0547	-0.0011	0.0155	-0.0442	0.0222	-0.0210
Perf. Measures			AIC = -4313.17		MSE = 0.0022		M. Dir = 96.7%	
4 to 8%	AL	0.0518	0.0088	0.0887	0.0608	-0.0141	-0.1239	0.0222
	GA	0.2097	0.1444	-0.1597	0.2736	0.1085	-0.1453	0.0614
	IL	-0.0704	0.0580	-0.0130	0.0637	-0.1461	0.0075	-0.1942
	MI	-0.1613	-0.0902	-0.1367	-0.0046	-0.1653	0.0213	-0.0050
	OK	-0.0728	0.0712	0.0812	0.1385	0.1349	0.1423	-0.0699
	SC	0.3048	0.2509	0.0757	0.3281	0.1094	-0.1411	-0.0681
	TN	0.2390	-0.2417	-0.1098	0.2492	0.0383	-0.2789	0.0549
	TX	0.0855	0.2925	0.0623	0.3199	-0.0566	-0.0627	0.0348
Avg.	0.0733	0.0617	-0.0139	0.1787	0.0011	-0.0726	-0.0205	
Perf. Measures			AIC = -4934.74		MSE = 0.0009		M. Dir = 96.1%	
Greater	CA	-0.0922	-0.2086	0.3866	-0.3866	-0.1163	-0.1468	0.0777

than 8%	CT	0.1911	0.1776	0.1274	0.3043	0.1327	-0.0605	0.1865
	DC	0.1551	0.1187	0.4381	0.0761	0.1635	0.0791	-0.1658
	MD	0.1768	0.2590	0.3278	0.1521	0.1295	-0.1718	0.1340
	NJ	0.3836	0.3622	0.6924	0.2850	0.0953	-0.2159	0.0631
	NY	0.2012	0.5001	0.5056	0.3671	0.0637	-0.0488	0.0273
	Avg.	0.1693	0.2015	0.4130	0.1330	0.0781	-0.0941	0.0538
	Perf. Measures	AIC = -5154.08		MSE = 0.0007		M. Dir = 95.8%		

Table 2: RANN spillover weight matrix.

4.4.2 Feature analysis: Average ensemble weights

Table 2 presents an average of the feature weights by the SALT category. In this section, we average these weights to create an ensemble average. Some highlights of the results are: a) on average daily municipal bond yields of all states are positively impacted by an AR(1) process, b) in the <4% and the 4% to 8%, the lagged US Returns negatively impact the individual state returns, c) consistency is further evidenced in the positive impact of the lagged SA returns, d) the COVID impact on state returns is negative in the <4% category but positive in the other SALT two categories, e) the precious metals impact is precisely the opposite of the COVID impact, and f) lastly, along with the lagged US Returns volatility, spillover into the states is negative in the <4% and 4% to 8% categories but positive in the >8% category.

4.5 Network feature map

The K4-RANN feature map (Fig. 4) shows the node transmission lines from each input feature (left boxes with rounded edges) to each labeled centroid (hidden nodes) in the neutral black color. The black lines represent the positive optimized weights, and the red lines represent the negative weights.

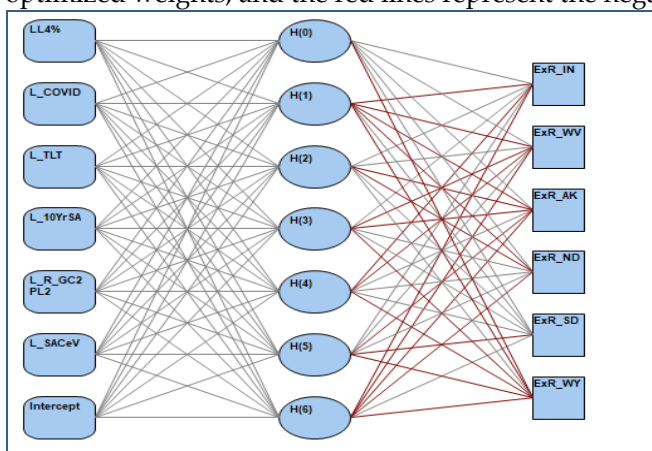


Fig. 4: Network feature map for the < 4% TCJA group

To demonstrate, utilizing the estimated model weights from table 2, in the <4% category, the estimated linear output function for state AK is stated as:

$$R_{AK,t} = -0.1462 + 0.0262\bar{R}_{t-1} - 0.2183R_{US,t-1} - 0.0914R_{SA,t-1} - 0.1139Covid_{t-1} + 0.3078GP_{t-1} - 0.2316\sigma_{SA,t-1}^2 + \epsilon_t, \tag{13}$$

4.6 Policy perspectives

Estimating an autoregressive spillover model reveals directional system parameters that can assist policy practitioners when making predictions for scarce resources. The analysis is presented in sections to explain how the effects of SALT, spillovers, and COVID-19 converge over the study period.

4.7 Feature analysis: The U.S. states and SA trade spillover

The following section examines the interaction among ranked total muni-trades, the export position, and the SALT tax category. To illuminate the value of the RANN weights, we summarize the signed weights within the interaction.

	Lagged States	Lagged USA	Lagged SA	Lagged COVID	Lagged GP	Lagged SA Vol	Rank Muni Trades	Trade Rank	TCJA Category
CA	-	+	-	-	-	+	1	4	>8%
NY	+	+	+	+	-	+	2	7	>8%
TX	+	+	+	-	-	+	3	1	4-8%
NJ	+	+	+	+	-	+	4	>10	>8%
IL	+	-	+	-	+	-	5	2	4-8%
MI	-	-	-	-	+	-	6	6	4-8%
GA	+	-	+	+	-	+	7	9	4-8%
MD	+	+	+	+	-	+	8	>10	>8%
CT	+	+	+	+	-	+	9	>10	>8%
IN	+	+	+	-	-	+	10	>10	<4%

Table 3: Interaction of RANN signed weights of 10 states with the highest muni trades (*Rank Muni Trades*) against the export rank position (*Trade Rank*) and SALT category (*TCJA Category*).

As seen in table 3, some noticeable contributions of the feature variables in the top 10 muni trading states' returns are:

- Based on ranking, the states of CA and NY have the most significant muni bond trades during the study period, but the feature variables have a very different impact on their returns. These two states are also in the >8% SALT category and are in the top 10 commodity exports to SA.
- Most feature variables positively impact the states' returns, as shown by the high amount of green on the heatmap.
- The precious metal impact is negative across all states except for IL and MI
- The SA volatility spillover provides the exact opposite of the precious metal effect. All states except IL and MI have a positive spillover effect.

Autoregressive contribution. Referencing table 2, in the >8% category, the AR(1) process is weighted positively across states except for CA. For the other two SALT categories <4% and 4% to 8%, all except three states (WY, MI, and TN) indicate a positive AR(1). The findings suggest a partial but disproportionate causal impact of the AR(1) contribution based on the TCJA tax effect. The geographical dispersion within these two categories also describes the disproportional impact of the TCJA.

SA government bond market volatility spillover. Spillover yield volatility from SA for states with the highest muni trading volume (Table 2) directly increases yields in all states except MI and CT. Bloomberg Fixed Income recently reported how the record demand at a recent South African weekly sale of government debt indicated a 'lure' for relatively high yields outweighing investors' concern about the country's fiscal path. The lack of focus on credit rating volatility and the rise of yields on hard currency bonds reflect the valuation uncertainty in SA bond markets. The estimating models identify the direction and magnitude of the volatility of SA spillover into U.S. muni markets.

The COVID-19 pandemic. The signed COVID-19 weights (Table 3) primarily support the Federal Reserve Bank of Kansas City's finding that "...the initial spike in muni yields was...due to a lack of liquidity in the market rather than state-specific credit risk" (Bi, Marsh, Dice, & Gulati, 2020). Considering the Reserve Bank analysis, the weighted coefficients of the COVID impact report a mixed effect. For example, except for CA, the COVID weights are all positive across states in the >8% category. But half of the states in the 4%-8% category are negative. And all but one of the weights in the <4% category are negative. The results presented here confirm a preliminary analysis by Sansa (2020). The author examined the impact of COVID-19 on the financial markets of the U.S. (New York Stock exchange) and China. The author reports that COVID-19 significantly impacted the financial markets from March 1, 2020, to March 25, 2020. The study findings are within the time frame of this analysis. Considering the FED report as cited, this study corroborates the COVID-19 impact on the financial performance across SALT states.

5 Summary and conclusions

In the face of U.S. regulatory efforts to mitigate COVID-19 effects, there is a question of whether global trading partners experienced similar government intervention to ally the negative impact of the pandemic. This study examined the spillover question under COVID-19. We proposed an econometric model that relied on an ML technique to map the COVID-19 effect on the network of muni bond return and volatility spillovers among U.S. SALT states and the South African bond market. The spillover system

of models utilized a unique database of approximately 11.5 million municipal bond trades. A methodology to transform the 'Big Data' muni database to daily price observations was implemented for parsimony with extant research. Regression weights were obtained by deploying an enhanced RANN. The algorithmic solution to the spillover model proved robust for algorithmic parameter control settings.

The study contributes several novel findings that describe muni trades through the COVID-19 period. Among SALT tax impacts on state-based muni trades, in the >8% category, we report that the AR(1) process is weighted positively across all East coast states during the global pandemic. However, For the other two categories <4% and 4% to 8% on average, AR(1) causality is negative in three states (WY, MI, and TN). The partial and disproportionate causal impact of AR(1) after the passage of the TCJA effect was previously undiscovered.

The COVID-19 pandemic may have temporarily worked with volatility spillover from South Africa to depress U.S. muni prices. The states of AK, WY, IL, and MI experience the adverse joint effects of these two events (i.e., negative coefficients in the respective columns of table 2). Conversely, GA, TN, CT, MD, NJ, and NY responded positively to the joint occurrence of the pandemic and volatility spillover from South Africa (i.e., positive coefficients in the respective columns of table 2). Interestingly, within the >8% category, only the CA and DC fail to show evidence of a joint effect (i.e., negative or positive).

Lastly, and interestingly, is the role of precious metal production. The lagged GP effect was evident across many of the SALT-impacted states. Only AK, ND, SD, IL, MI, OK, and DC present positive coefficients. These states are committed to a mining industry that includes exploration, mine development, and mineral production. The absence of South African competition across these states is a likely reason for the estimated signs.

References

- Ando, S. (2019). *International Financial Connection and Stock Return Comovement* (IMF Working Paper: WP/19/181). Retrieved from IMF:
- Bi, H., Marsh, W. B., Dice, J., & Gulati, C. (2020). *Understanding the Recent Rise in Municipal Bond Yields*. Economic Bulletin. Federal Reserve Bank of Kansas City.
- Bianchi, D., Büchner, M., & Tamoni, A. (2021). Bond Risk Premiums with Machine Learning. *The Review of Financial Studies*, 34(2), 1046-1089. doi:<https://doi.org/10.1093/rfs/hhaa062>
- Bollerslev, T. (1986). Generalized Autoregressive Conditional Heteroskedasticity. *Journal of Econometrics*, 31, 307-327.
- Chiu, T. (2019). *Understanding Generalized Whitening and Coloring Transform for Universal Style Transfer*. Paper presented at the 2019 IEEE/CVF International Conference on Computer Vision (ICCV), Seoul, Korea.
- Dash, G. H., Kajiji, N., & Vonella, D. (2018). The role of supervised learning in the decision process to fair trade U.S. Municipal debt. *Euro Journal on Decision Processes*(Financial Decision Support). doi:10.1007/s40070-018-0079-2
- Dash Jr., G. H., & Kajiji, N. (2008). Engineering a Generalized Neural Network Mapping of Volatility Spillovers in European Government Bond Markets. In C. Zopounidis, M. Doumpos, & P. M. Pardalos (Eds.), *Handbook of Financial Engineering* (Vol. 18): Springer.
- di Giovanni, J., & Hale, G. (2021). *Stock Market Spillovers Via the Global Production Network: Transmission of U.S. Monetary Policy*. NBER Working Paper No. w28827, Available at SSRN: <https://ssrn.com/abstract=3851830>.
- Dizioli, A., Guajardo, J., Klyuev, V., Mano, R. C., & Raissi, M. (2016). *Spillovers from China's Growth Slowdown and Rebalancing to the ASEAN-5 Economies* (IMF Working Paper No. 16/170). Retrieved from <https://ssrn.com/abstract=2882607>
- Engle, R. F. (1982). Autoregressive Conditional Heteroskedasticity with Estimates of the Variance of U.K. Inflation. *Econometrica*, 50, 987-1008.
- Erling, M. (2016). *Analyzing Precious Metals Returns Using a Kalman Smoother Approach*. Retrieved from SSRN: <https://ssrn.com/abstract=2827061>:
- Góes, C., Kamil, H., de Imus, P., Garcia-Escribano, M., Perrelli, R., Roache, S., & Zook, J. (2017). *Spillovers from U.S. Monetary Policy Normalization on Brazil and Mexico's Sovereign Bond Yields* (IMF Working Paper No. 17/50). Retrieved from <https://ssrn.com/abstract=2958201>:
- Kristjanpoller, W., & Minutolo, M. C. (2016). Forecasting volatility of oil price using an artificial neural network-GARCH model. *Expert Systems with Applications*, 65, 233-241.
- Lahmiri, S. (2017). Modeling and Predicting Historical Volatility in Exchange Rate Markets. *Physica A: Statistical Mechanics and its Applications*, 471, 387-395.

- Le, T. N., & Kakinaka, M. (2010). International Transmission of Stock Returns: Mean and Volatility Spillover Effects in Indonesia and Malaysia. *Global Journal of Business Research*, 4(1), 115-131. Retrieved from <http://ssrn.com/abstract=1633088>
- Leon-Delgado, H. d., Praga-Alejo, R. J., Gonzalez-Gonzalez, D. S., & Cantú-Sifuentes, M. (2018). Multivariate statistical inference in a radial basis function neural network. *Expert Systems with Applications*, 93, 313-321. doi:<https://doi.org/10.1016/j.eswa.2017.10.024>
- Mademlis, D. K., & Dritsakis, N. (2021). Volatility Forecasting using Hybrid GARCH Neural Network Models: The Case of the Italian Stock Market. *International Journal of Economics and Financial Issues*, 11(1), 49-60.
- Nelson, D. B. (1991). Conditional Heteroskedasticity in Asset Returns: A New Approach. *Econometrica*, 59, 347-370.
- Prathiba, R., BalasinghMoses, M., Devaraj, D., & Karuppasamypandiyana, M. (2016). Multiple Output Radial Basis Function Neural Network with Reduced Input Features for On-line Estimation of Available Transfer Capability. *Control Engineering and Applied Informatics*, 18(1), 95-106.
- Raman, N., & Leidner, J. L. (2018). Municipal Bond Pricing: A Data Driven Method. *International Journal of Financial Studies*.
- Rigobon, R. (2002). *International Financial Contagion: Theory and Evidence in Evolution*. The Research Foundation of the Association for Investment Management and Research. Charlottesville, VA,.
- Roy, R. P., & Roy, S. S. (2017). Financial contagion and volatility spillover: An exploration into Indian commodity derivative market. *Economic Modelling*, 67, 368-380. doi:<https://doi.org/10.1016/j.econmod.2017.02.019>
- Rudenko, O., & Bezsonov, O. (2011). Function Approximation Using Robust Radial Basis Function Networks. *Journal of Intelligent Learning Systems and Applications*, 3, 17-25. Retrieved from <http://www.SciRP.org/journal/jilsa>
- Sammartino, F., Stallworth, P., & Weiner, D. (2018). *The Effect of the TCJA Individual Income Tax Provisions across Income Groups and across the States*. Retrieved from Tax Policy Center: Urban Institute & Brookings Institution
- Sansa, N. (2020). The Impact of the COVID - 19 on the Financial Markets: Evidence from China and USA. *Electronic Research Journal of Social Sciences and Humanities*, 2(II).
- Shahzad, S. J. H., Bouri, E., Kang, S. H., & Saeed, T. (2021). Regime specific spillover across cryptocurrencies and the role of COVID-19. *Financ Innovation*, 7(5). doi:<https://doi.org/10.1186/s40854-020-00210-4>
- Shehzad, K., Xiaoxing, L., Bilgili, F., & Koçak, E. (2021). COVID-19 and Spillover Effect of Global Economic Crisis on the United States. *Financial Stability. Frontiers in Psychology*. doi:<https://doi.org/10.3389/fpsyg.2021.632175>
- Urom, C., Anochiwa, L., Yuni, D., & Idume, G. (2019). Asymmetric linkages among precious metals, global equity and bond yields: The role of volatility and business cycle factors. *The Journal of Economic Asymmetries*, 20, 1-25.
- Vuyyuri, S., & Mani, G. S. (2005). Gold Pricing in India: An Econometric Analysis. *Journal of Economic Research*, 16(1).
- Wang, Q., & Xinyu, H. (2021). Spillover effects of the United States economic slowdown induced by COVID-19 pandemic on energy, economy, and environment in other countries. *Environmental Research*, 196.
- Wu, Y., Wang, H., Zhang, B., & Du, K.-L. (2012). Using Radial Basis Function Networks for Function Approximation and Classification (Publication no. <https://doi.org/10.5402/2012/324194>). (Article ID 324194).